High Pressure Ignition and Combustion of Aluminum Hydride

Gregory Young[a], Rohit Jacob[b] & Michael R. Zachariah[b]

[a] Naval Surface Warfare Center-Indian Head Division, RDT&E
Department, Indian Head, Maryland, USA

[b] University of Maryland, College Park, Maryland, USA
Accepted author version posted online: 09 Apr 2015.

Click for updates

PLEASE SCROLL DOWN FOR ARTICLE

Taylor & Francis
Taylor & Francis Group

HIGH PRESSURE IGNITION AND COMBUSTION OF ALUMINUM HYDRIDE

Gregory Young,[1] Rohit Jacob,[2] and Michael R. Zachariah[2]

[1]*Naval Surface Warfare Center–Indian Head Division, RDT&E Department, Indian Head, Maryland, USA*
[2]*University of Maryland, College Park, Maryland, USA*

An experimental study was conducted to determine the high pressure ignition characteristics of α-aluminum hydride. Aluminum hydride particles were heated on a platinum filament at heating rates of approximately 1×10^5 K/s in a pressure vessel for pressures ranging up to about 7 MPa, in order to quantify the ignition temperature and to observe the ignition process. Experiments were conducted in air, argon, and nitrogen as the pressurizing environment. This study revealed that the dehydrogenation of aluminum hydride is not a function of pressure under the conditions tested. In addition, ignition temperatures were found to be approximately linearly related to pressure until pressures exceeded about 0.4 MPa, at which point they remained constant through the highest pressures tested. High speed imaging of the ignition process showed a dramatic change in the ignition behavior for pressures above 0.4 MPa, corresponding to what we believe is a threshold for H_2/air autoignition or perhaps even an explosion limit. We find that the combustion behavior of aluminum hydride particles shared many traits similar to what has been previously observed with aluminum particles including a diffusion flame surrounding the particle, spinning, jetting, and explosions/fragmentation. Quenched particles also showed clear evidence of gas phase combustion with parent particles containing nanofeatures, which were condensed from the gas phase. The results of this study provide additional understanding on the ignition and combustion process of aluminum hydride at extreme conditions, which may be useful in modeling efforts or in the development of solid propellants.

INTRODUCTION

Metal hydrides are of great interest as both hydrogen storage media (Ahluwalia, 2009; Graetz and Reilly, 2005, 2006; Graetz et al., 2007; Ismail and Hawkins, 2005; Sakintuna et al., 2007; Sartori et al., 2009) and as fuel supplements in propulsion systems (Connell et al., 2011; Deluca et al., 2007; Shark et al., 2013; Young et al., 2010a, 2010b). As hydrogen storage media, several metal hydrides offer greater storage density than liquid hydrogen (Sakintuna et al., 2007). For rocket propulsion systems some metal hydrides, specifically aluminum hydride, when used as a fuel supplement can significantly

increase the specific impulse of a system while at the same time reducing the flame temperature (Connell, 2011; Deluca, 2011; Young, 2010a, 2010b) of the propellant.

In general there are three competing models that attempt to describe metal hydride decomposition characteristics: (1) shrinking core, (2) nucleation and growth, and (3) multistep kinetics. In one theoretical study presented by Castro and Meyer (2002) in which hydrogen desorption was characterized by thermal desorption spectroscopy, four alternative rate limiting steps for metal hydride dehydrogenation were identified: (1) bulk diffusion, (2) phase transformation, (3) bulk to surface transfer, and (4) H–H surface recombination. In general, these steps are based on thermal gravimetric analysis (TGA) or differential scanning calorimetry (DSC), which operate at heating rates on the order of tens of degrees per minute. On the other hand, steady state combustion processes, such as in propellant burning, experience particle heating rates in excess of ~100,000 K/s. It is reasonable to assume then, that the physical-chemical processes at high heating rate conditions may involve different rate limiting processes than those encountered under the low heating rate experimental studies.

The decomposition characteristics of aluminum hydride have been studied extensively (Bazyn, 2007; Graetz and Reilly, 2005, 2006; Graetz et al., 2007; Ismail and Hawkins, 2005; Young et al., 2010a) demonstrating that the dehydrogenation of aluminum hydride occurs at temperatures as low as ~160°C depending on the heating rate and synthesis method. Previous studies on aluminum hydride dehydrogenation (Bazyn et al., 2007; Graetz and Reilly, 2005, 2006; Graetz et al., 2007; Ismail and Hawkins, 2005; Young et al., 2010a) have been conducted at atmospheric pressure or below, leaving a gap in our knowledge of dehydrogenation at elevated pressures. The only recent reports of high pressure work is that of Bazyn et al. (2004) who studied the combustion behavior of aluminum hydride at elevated pressures, but quantification of dehydrogenation characteristics was not reported. It is documented that upon dehydrogenation, amorphous and/or crystalline aluminum remains (Bazyn et al., 2007), which combusts on time scales similar to that of similarly sized aluminum (Bazyn et al., 2004).

In our previous study (Young et al., 2010a), we found that the ignition temperature of aluminum hydride was comparable to that of nanoaluminum, and a function of heating rate while oxidizing species had no impact on the ignition temperature. Furthermore, we found that at heating rates relevant to propellant combustion, the rate controlling process for dehydrogenation was limited by intraparticle diffusion to hydrogen evolution, rather than the intrinsic kinetics of Al–H bond breaking. In this study we focus on the ignition behavior of aluminum hydride under elevated pressure.

METHOD OF APPROACH

The aluminum hydride studied in this effort was α-aluminum hydride, which is the most thermally stable phase of aluminum hydride. The methods for synthesis and stabilization of the as received α-aluminum hydride used in the study are not fully known to us, however, this is the same material used in previous efforts (Connell et al., 2011; Young et al., 2010a, 2010b) and we believe it is likely to be the same material as studied by both Ismail and Hawkins (2005) and Bazyn et al. (2004, 2007). Representative particles are shown in Figure 1 in a scanning electron microscope (SEM) image. The particles are rhombohedral crystals, and were sieved to range from 20 μm to 32 μm. In each of the subsequently described experiments, the metal hydrides were dispersed in hexane from
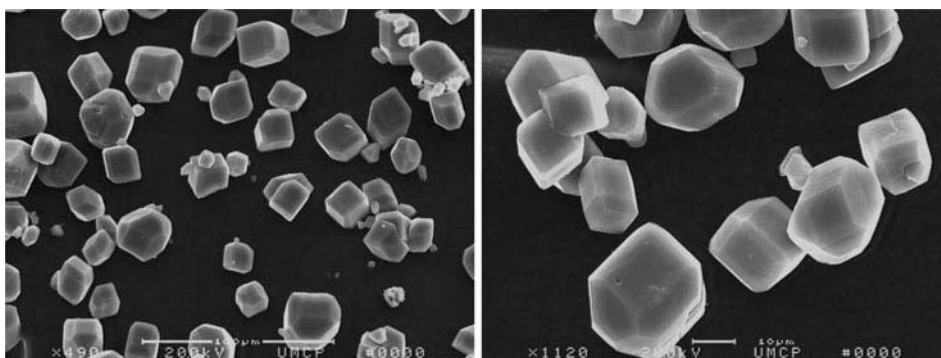
Figure 1 Scanning electron microscope images of aluminum hydride.

which the samples were drawn into a syringe, deposited on an ~75-μm-diameter platinum filament, and given sufficient time to air dry.

Heated Filament Experiments

In our previous work (Young et al., 2010a), we studied the dehydrogenation and ignition process of aluminum hydride at heating rates up to ~6 × 10^5 K/s by a custom designed temperature jump (T-Jump) probe coupled with a Time of Flight Mass Spectrometer. For this study we limited heating rates to ~1 × 10^5 K/s and focused on the effects of pressure on the ignition process. We systematically varied pressure from atmospheric to about 7 MPa by placing heating filaments (75-μm platinum wire) into a 0.1-liter pressure vessel rated to 24.1 MPa and used the same T-Jump ignition system as in our previous study (Young et al., 2010a).

The pressure vessel had three quartz windows providing optical access. Two windows were located at the same vertical height as the heating filament, and a third window was located at the bottom of the pressure vessel looking upward at the sample. The T-Jump pressure vessel assembly can be seen schematically in Figure 2. Pressure was monitored and recorded with a Setra Model 206 static pressure transducer. A K-type thermocouple was also installed in the pressure vessel to ensure that samples would not be significantly heated by adiabatic compression during the pressurization process. The highest temperature rise associated with the pressurization process was about 5 K.

Experiments were conducted with air, argon, and nitrogen as pressurizing gases. Air was selected as the gas of study for an oxidizing environment. Since nanoaluminum had previously been observed to combust in nitrogen (Son et al., 2003), and our previous study on aluminum hydride (Young et al., 2010a) found similar ignition characteristics to nanoaluminum; nitrogen was considered as well. Finally, experiments were carried out in argon to provide a comparison in a purely inert atmosphere of particle dynamics upon decomposition. Two Hamamatsu model H7827-012 photomultiplier tubes (PMTs) were used to monitor broadband light emission in real-time to characterize ignition, with the output sent directly to an oscilloscope. The PMTs had a spectral range of 300–850 nm. Ignition was defined as 2% maximum light intensity collected by the PMTs as in our
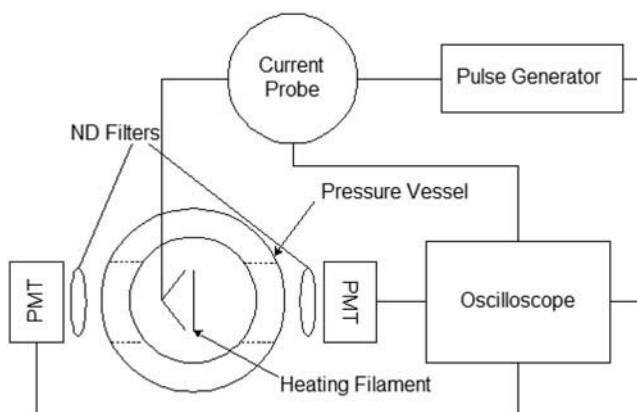
Figure 2 Schematic diagram of high pressure T-jump setup.

previous study (Young et al., 2010a). In addition, high speed imaging with and without backlighting was employed to provide further details on the ignition and combustion process of the metal hydrides.

During the ignition experiments, the input voltage and resulting current were monitored, and for a known length of the platinum wire, the temperature-time history was determined from the wire resistance using the Callendar-Van Dusen equation:

$$\frac{R}{R_o} = 1 + \alpha T + \beta T^2 \tag{1}$$

where $\alpha = 3.91 \times 10^{-3}$, $\beta = -5.78 \times 10^{-7}$, and R_o is the reference resistance obtained from the length of the wire at ambient temperature.

RESULTS AND DISCUSSION

Decomposition Characteristics

In our previous study (Young et al., 2010a), we examined the dehydrogenation process of aluminum hydride under vacuum conditions by Time of Flight Mass Spectrometry. At that time we determined that dehydrogenation was clearly a function of heating rate, and at heating rates characteristic of propellant combustion, the rate controlling process for dehydrogenation was not the intrinsic kinetics of Al–H bond breaking but rather an intraparticle diffusion limit (Young et al., 2010a). To further demonstrate this behavior we subjected a sample to high heating rates (~1 × 10^5 K/s) under vacuum with our T-Jump apparatus for post mortem inspection. Figure 3 shows SEM images of aluminum hydride samples heated to various temperatures. At approximately 750°C the particles appear highly porous, with some evidence of melting of the smaller particles. At approximately 1100°C, the particles show clear evidence of melting. Ismail and Hawkins (2005) also conducted SEM analysis of partially and fully decomposed aluminum hydride after vacuum thermal stability experiments conducted at 60°C over a period of days. Interestingly the partially decomposed sample showed some
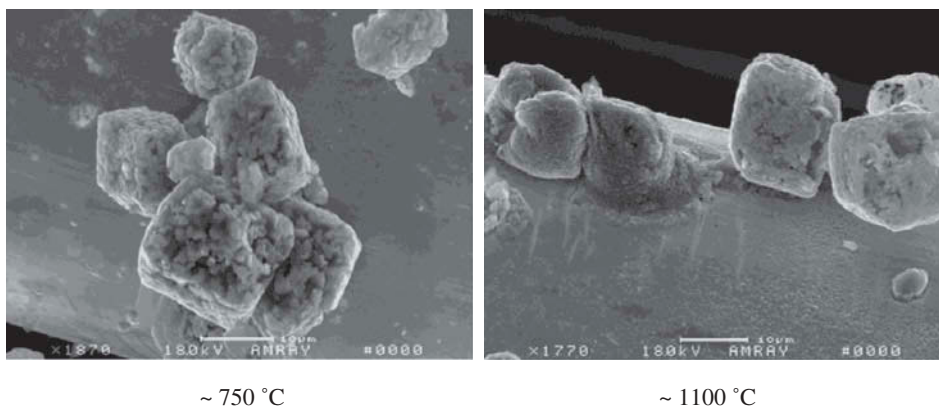
~ 750 ˚C   ~ 1100 ˚C

Figure 3 SEM image of aluminum hydride heated to various temperatures under vacuum conditions.

porosity and cracking but not nearly to the same extent as our samples, which were subjected to very high heating rates, but for heating times several orders of magnitude shorter. Not surprisingly, since Ismail and Hawkins' (2005) heating was well below the melting point, the samples remained relatively crystalline, while our samples appear to lose their structure. Unfortunately, we cannot quantify the extent of decomposition of our samples by typical thermal analysis techniques due to sample size limitations. However, we expect that they are very nearly fully decomposed if not fully decomposed, based on our prior work (Young et al., 2010a) in which hydrogen was released at temperatures between 650–1100 K depending on the heating rate. Ismail and Hawkins' (2005) fully decomposed samples showed no porosity and maintained their original shapes with an approximate size reduction of 20–30% leaving behind a cubic shaped aluminum particle.

Determination of Ignition Temperature

Ignition temperature was determined using the broadband light emission signal from two PMTs using 2% maximum light intensity as the threshold definition of ignition as in our previous study (Young et al., 2010a). A background signal, with a bare heating filament and no sample, was taken for each experiment and subtracted off of the raw signal in the determination of ignition temperature. Figure 4 provides representative optical emission for atmospheric (0.101 MPa) and elevated pressure conditions (5.3 MPa), which clearly shows distinct differences. At elevated pressures, the optical emission is highly fluctuating, and does not achieve the same peak intensity of the atmospheric pressure case, which has a much smoother and symmetric emission profile. In general, we observed this smooth emission behavior until we exceeded about 0.3 MPa at which point the signal became erratic as seen in the example given in Figure 4. In addition, the initial rate of signal intensity rise is significantly increased at elevated pressures suggesting an increase in reaction rate. However, the overall duration of signal intensity is comparable between atmospheric and elevated pressure conditions. This result is not surprising since the Beckstead Correlation (Beckstead, 2005) implies that the overall burning time of aluminum particles is at best a weak function of pressure, and several experimental and numerical studies support that conclusion (Bazyn et al., 2005; Belyaev et al., 1968; Frolov et al., 1972; Kuryavtsev et al., 1979; Law, 1973). Although there is evidence to suggest that any pressure dependency
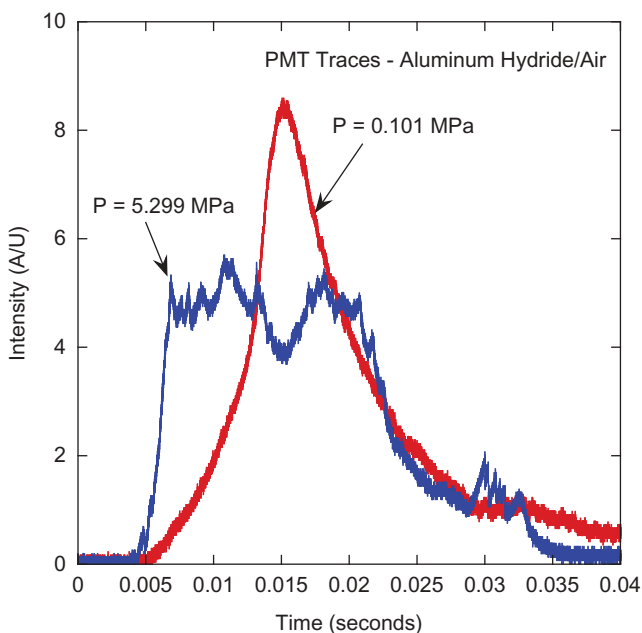
Figure 4 PMT traces of aluminum hydride/air ignition at two pressures.

is somewhat dependent on oxidizer type (Bazyn et al., 2005). Particles of the size used in this study would be expected to be diffusion controlled during combustion. Since the diffusion of oxidizer to the particle is proportional to the product of density (proportional to pressure) and the diffusion coefficient (inversely proportional to pressure), the overall process should be independent of pressure (Bazyn et al., 2005).

Figure 5 shows results of the measured ignition temperature in air with pressures ranging from atmospheric up to about 7 MPa. Typically, three experiments were conducted at each condition in order to provide a measure of repeatability. At atmospheric pressure the ignition temperatures were consistent with our previous study (Young et al., 2010a) at about 900 K for a heating rate of $\sim 1 \times 10^5$ K/s. As the pressure was increased to about 0.4 MPa, we observed an approximately linear decrease in the ignition temperature to about 800 K. Beyond about 0.4 MPa the ignition temperature appears to be relatively independent of pressure, holding just below 800 K.

Although nanoaluminum has been shown to ignite and propagate in a nitrogen only atmosphere (Son et al., 2003), and AlN was detected in X-ray diffraction (XRD) by Il'in et al. (2001) in combustion products of aluminum hydride and air, all attempts to ignite aluminum hydride in a nitrogen only environment were unsuccessful.

High-Speed Imaging

During our first series of experiments, we employed a Phantom 7.3 high-speed camera to observe the low (0.1 MPa) and high pressure (~ 7 MPa) ignition process of aluminum hydride for heating rates of approximately 1×10^5 K/s. Images were taken at a rate of 21,052 frames per second for all experiments. Figure 6 shows a sequence
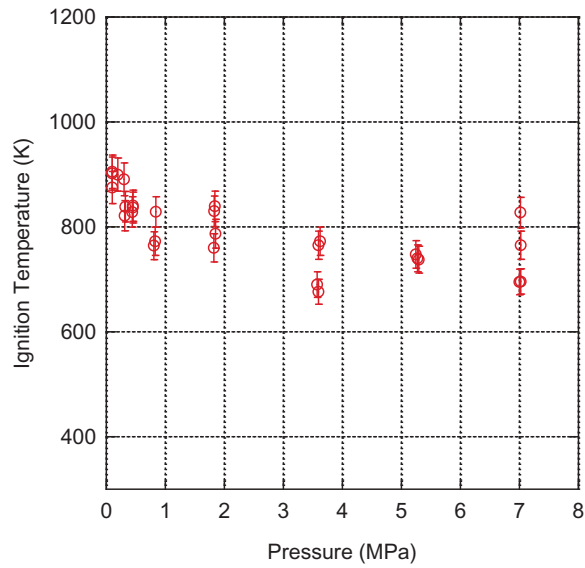
Figure 5 Ignition temperatures of aluminum hydride in air as a function of pressure (heating rate of ~1 × 10⁵ K/s).

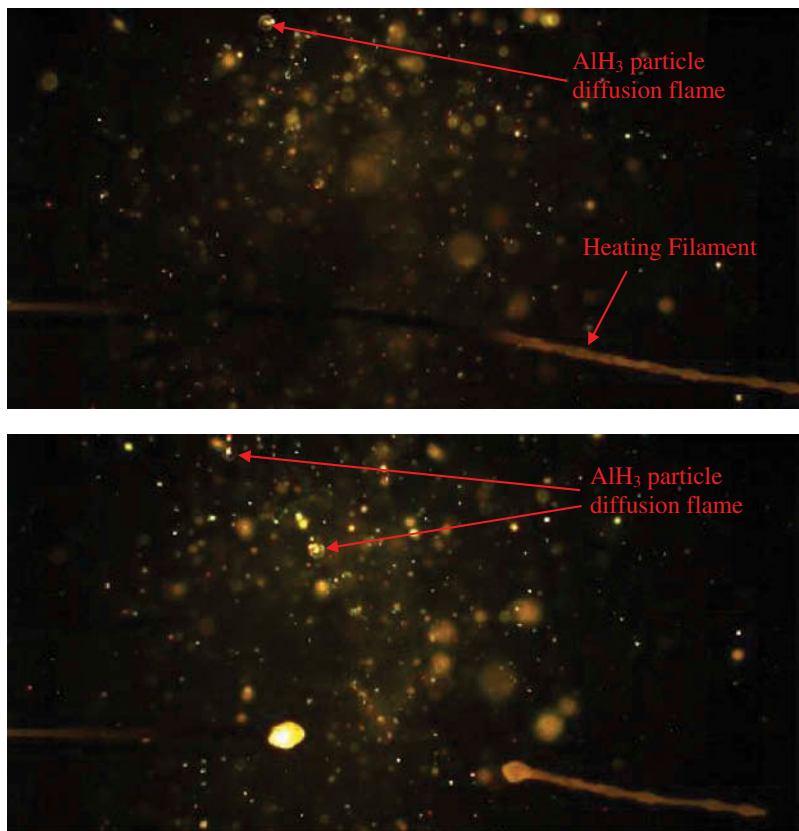**Figure 6** Aluminum hydride ignition in air (0.101 MPa with a heating rate of ~1 × 10⁵ K/s).

of images of aluminum hydride igniting at 0.101 MPA (1 atm) in air. Particles were observed leaving the heating filament approximately symmetrically, and igniting in the surrounding gas. It was also possible to observe diffusion flames surrounding the particles similar to that observed for aluminum particles (Brzustowski and Glassman, 1964; Bucher et al., 1996, 1998, 1999; Frolov et al., 1972). In addition, individual particles also demonstrated jetting and spinning phenomenon, which is also similar to that of aluminum (Drew et al., 1964; Frolov et al., 1972; Gordon et al., 1968; Macek, 1967). During burning, ejections of smaller burning material were commonly observed, along with some instances of particle explosions. These observations are highly consistent with pressure build-up of hydrogen within the particle that had not escaped the particle prior to ignition. However, particle explosion or fragmentation has also been observed in previous studies on aluminum particle combustion (Friedman and Macek, 1963; Frolov et al., 1972; Gordon et al., 1968). Although it should be pointed out that in those previous works the concentration of oxygen in the system were higher leading to a more vigorous burning possibly causing superheating of the liquid aluminum droplet leading to fragmentation. Under our conditions we did not observe ignition with similar sized aluminum. We attribute the reason particles leave the wire and burn, to hydrogen evolution, which acts to detach particles from the wire. Similar studies using nanoaluminum show ignition and burning only on the wire.

Figure 7 is a sequence of images, which shows the ignition process of aluminum hydride at about 3.6 MPa in air. The reference time shown in these images as well as in Figures 8 and 9, t_o, is the time at which the event being visualized is beginning. Due to the increased brightness, the exposure time of the camera was reduced to 1/5, with other camera settings remaining the same. The images show that the particles on the outermost part of the heating filament ignite first, and the reaction propagates inward on the wire meaning that not all particles were igniting at the same times. In addition, the particle dispersion is much more constrained compared to the 0.101 MPa condition, and they rise collectively from buoyancy forces. While the general characteristics of burning are similar to the lower pressure condition, the jetting behavior was more clearly pronounced and a remnant dense but fine smoke cloud was present that was not observed at lower pressures. This may in part be a result of the higher pressure condition leading to a higher adiabatic flame temperature than the lower pressure condition. For example, using the NASA CEA computer code (McBride and Gordon, 1996), the calculated adiabatic flame temperature of a stoichiometric mixture of aluminum hydride in air at 0.1 MPa is 2980 K compared to 3277 K at 3.6 MPa. While the vaporization temperature of aluminum increases with pressure, the vapor pressure is not a function of pressure. Thus, the partial pressure of aluminum in vapor at equilibrium is independent of pressure. Therefore, the higher flame temperature at higher pressures would be expected to promote greater vaporization of aluminum. Higher concentrations of vapor phase product species (alumina precursors) will result in higher nucleation rates, and thus a finer particle size distribution. This is consistent with the observed high density smoke cloud at higher pressures.

Figure 8 shows a sequence of images taken when backlighting was employed for the 0.1 MPa condition in air, with the same camera settings as in Figure 7. The backlit images show particles leaving the heating filament, some of which were much smaller than could be reasonably resolved with the current setup, and some of which were relatively large agglomerates. With backlighting a smoke cloud can now be readily observed.

Figure 9 provides shadowgraph images from backlighting at 3.6 MPa. Very apparent from these images are the density gradients that appear, which are highly consistent with
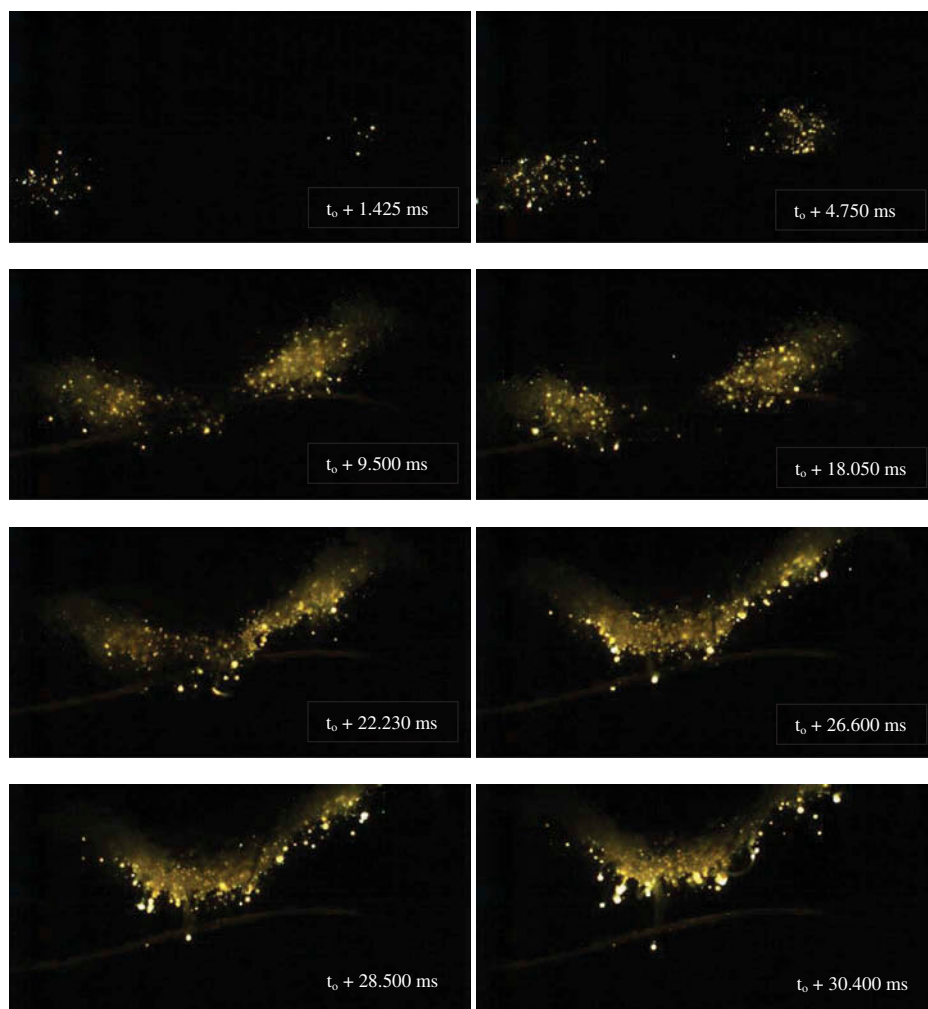
Figure 7 Aluminum hydride ignition in air (3.6 MPa with a heating rate of 1×10^5 K/s).

hydrogen generation and did not appear when nanoaluminum was used. Particles that have not yet reached ignition can be seen leaving the heating filament and igniting within the density gradient. To explore the role of hydrogen in the ignition process as a co-fuel, repeat experiments with argon (replacing air) showed density gradients in the shadowgraphs, but were significantly muted relative to the air case. This implies that hydrogen is clearly participating in the combustion process as a fuel to cause a local temperature increase and a lower density. The argon experiment also revealed that particles only leave the surface in the presence of air, implying that it is the combustion reaction of hydrogen with air that causes lift off. The images in Figure 9 reveal that the remaining aluminum after dehydrogenation is reacting within the products of H_2/air, namely, water vapor at some finite distance from the heating filament, as well as the surrounding air. It should be noted that we cannot be certain at this point whether it is a requirement for all the hydrogen to be released prior to aluminum ignition although it seems likely to be the case given the difference in reactivity
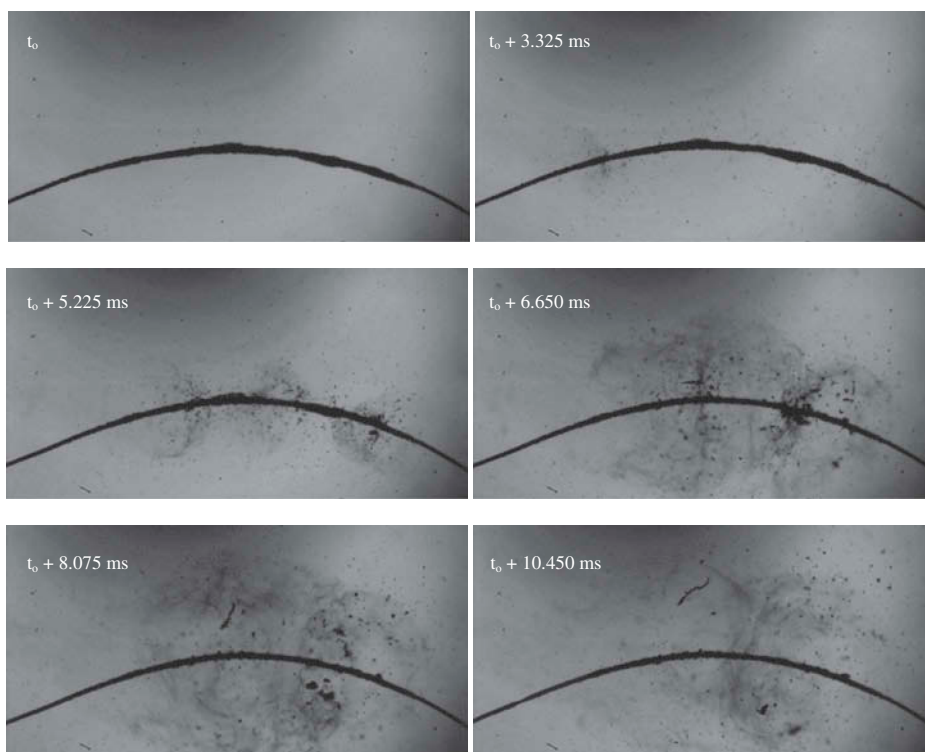
Figure 8 Backlit images of aluminum hydride ignition in air (0.101 MPa with a heating rate of 1×10^5 K/s).

between hydrogen gas and aluminum. The shadowgraph images also allow for very clear visualization of the smoke trails and jetting that were observed earlier.

Post-Combustion Particle Inspection

To evaluate the products of combustion, SEM stages were placed approximately 2.5 mm from the heating filament to capture and quench particles for post-combustion inspection. Figure 10 shows representative images from an experiment conducted at 0.1 MPa. The top image in Figure 10 shows a particle that is approximately 20 μm in diameter with numerous nanofeatures attached to its surface. The bottom image of Figure 10 is a zoomed-in image of one of the edges of the particle showing two distinct classes of particles that are associated with the nanofeatures. The first class are very fine particles <50 nm, while the second are well-defined spheres on the order of a few hundred nanometers. The smaller nanofeatures obviously must be formed from vapor phase condensation of the products of combustion (alumina), while the larger nanofeatures are a result of coalescence of the smaller nanofeatures. The larger particles can only grow as long as the temperature of the particle remains sufficiently high that they are above the particle melting point; i.e., of aluminum oxide. Once the parent particles cool sufficiently sintering is arrested and the primary particle size is frozen-in. Prior to ignition and combustion the particles were rhombohedral in shape and were sieved to between 20 and 32 μm. The captured particle is spherical and ~5 μm implying that the
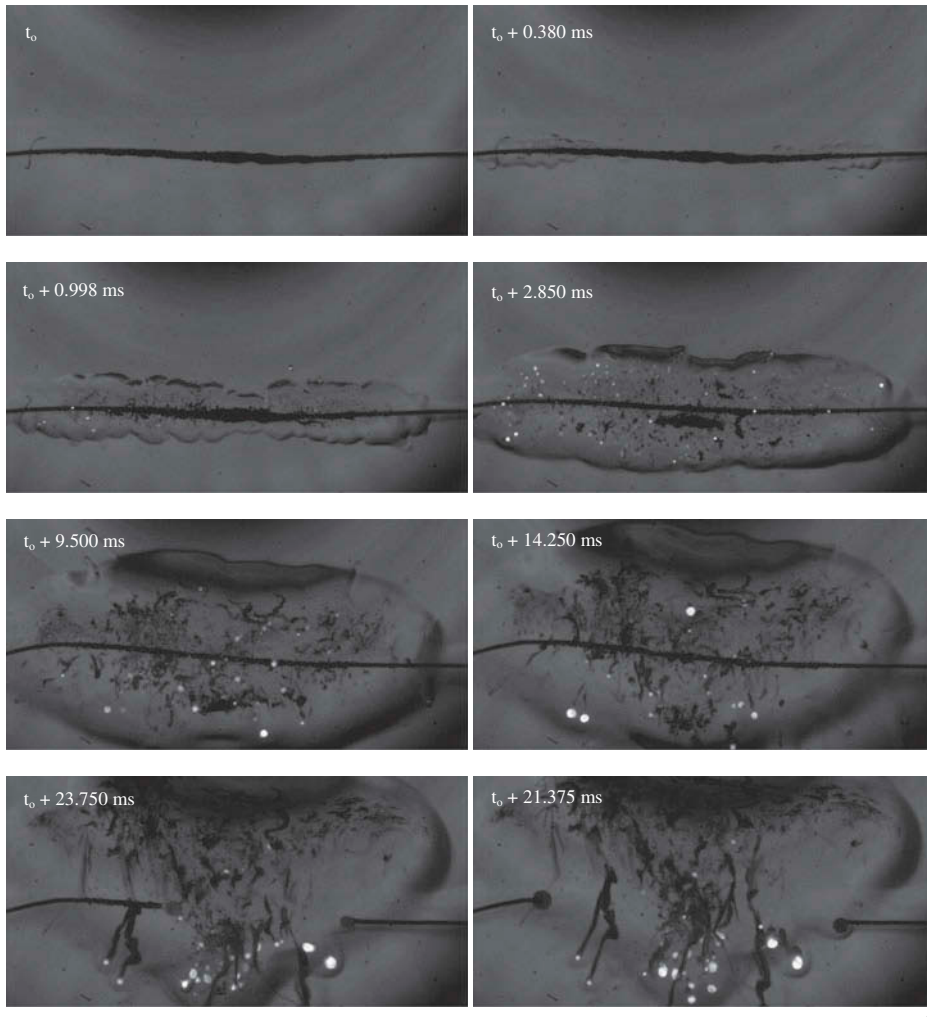
Figure 9 Backlit images of aluminum hydride ignition in air (3.6 MPa with a heating rate of 5×10^5 K/s).

particle experienced a molten state during burning, with most of the particle being consumed prior to quenching, and little or no particle-particle interactions occurring post-quench.

Figure 11 shows representative images of particles that were ignited and combusted at elevated pressure (3.6 MPa). Once again spherical parent particles are observed with surface decorated nanofeatures (Figure 11, top). The bottom image of Figure 11 shows the nanofeatures in detail, which are consistent with the larger spherical nanofeatures observed in the lower pressure ignition experiment. At this elevated pressure we did not observe the fine nanofeatures. This is consistent with higher pressures having higher adiabatic flame temperatures, which leads to more sintering in the fine particles.
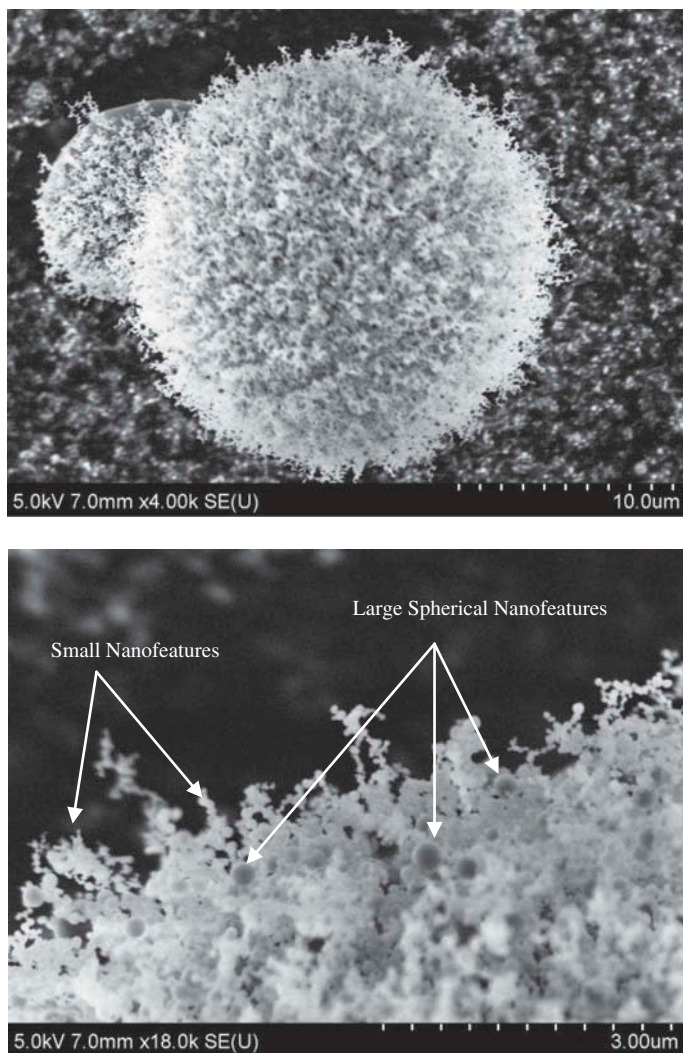
Figure 10 Aluminum hydride particles captured post combustion (0.101 MPa) (top: particle with two types of nanofeatures; bottom: zoomed-in image of particle showing two types of nanofeatures).

Discussion

The fact that the ignition temperature is more or less constant above about 0.4 MPa suggests that the temperature at which hydrogen is released is independent of pressure. The average ignition temperature, shown in Figure 5, above 0.4 MPa is 760 K, which is in reasonable agreement with our previous study (Young et al., 2010a) under vacuum conditions, where we found that the hydrogen release temperature for a heating rate of $\sim 1 \times 10^5$ K/s was about 720 K. We previously established that the dehydrogenation process of aluminum hydride is transport limited (Young et al., 2010a) at high temperatures and heating rates. Once chemical bond dissociation takes place a simple analysis
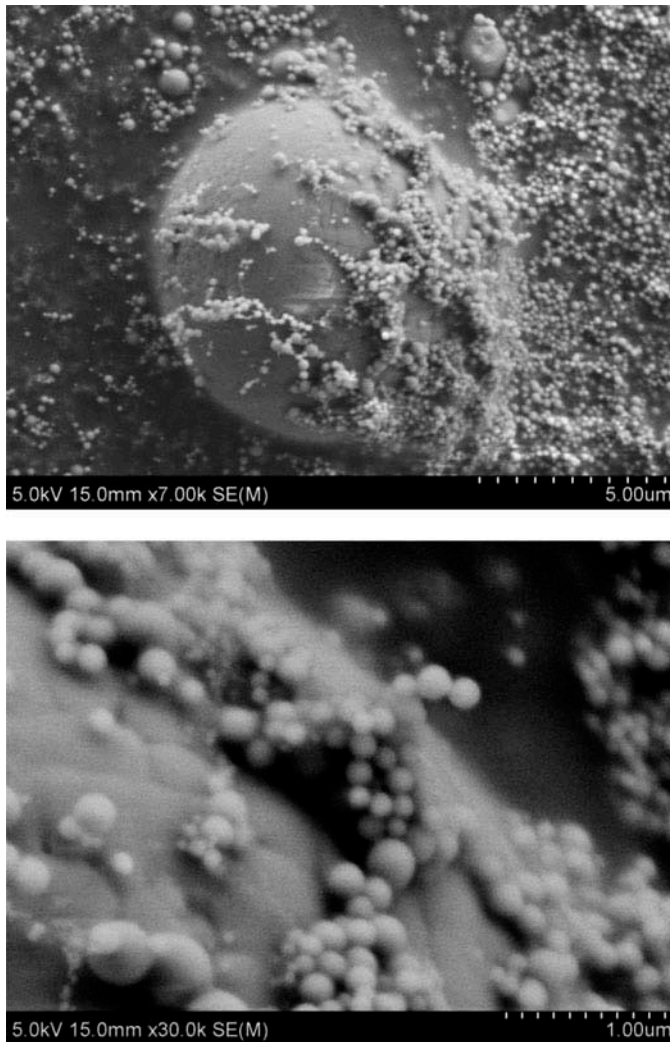
Figure 11 Aluminum hydride particles captured post combustion (3.6 MPa) (top: parent particle with attached nanofeatures; bottom: zoomed-in image showing nanofeatures).

reveals that there would be no further transport barrier to the dehydrogenation process under the conditions tested in this study. If one considers a 20-μm particle, which contains 10% by mass hydrogen, the calculated pressure of the gas occupying a 20-μm particle is on the order of hundreds of MPa. This is at least two orders of magnitude higher than the operating pressures considered in this study, and therefore one should not expect any dependence on pressure for the dehydrogenation process.

Ordinarily one would not expect the ignition temperature of solid particles to be affected by pressure since pressure mainly effects gas phase ignition and kinetics. However, in the case of metal hydrides, after decomposition, hydrogen is available for reaction and subjected to effects of pressure. Ignitability of hydrogen is enhanced with increasing pressure, meaning temperature requirements are reduced (Hu et al., 2009;

Kruetz and Law, 1996; Lewis and Von Elbe, 1987; Zheng and Law, 2004). In addition, under appropriate conditions, explosion of hydrogen gas with oxygen or air becomes more likely at increased pressure (Hu et al., 2009; Kruetz and Law, 1996; Lewis and Von Elbe, 1987; Zheng and Law, 2004). The initial decrease in ignition temperature of aluminum hydride can be explained by the increased ignitability of hydrogen at elevated pressures up to 0.4 MPa. The constant ignition temperature above 0.4 MPa can have two possible explanations. First, the kinetics of the H_2/air reaction may be faster than the resolution of our diagnostics, such that any differences are negligible. The second possibility is that the explosion limits of the H_2/O_2 reaction may have been reached. In either case, after dehydrogenation, there is a very minimal delay before the reaction of hydrogen/air occurs resulting in a constant ignition temperature over a wide range of pressures. The emission traces shown in Figure 4 and the gaseous structures observed in the shadowgraph images of Figure 9 further substantiate that the reaction kinetics increase significantly once a pressure threshold is reached. In fact, these two behaviors were observed to coincide suggesting a shift in reaction mechanism.

Both high speed imaging and the quenched particles shown in Figures 10 and 11 provide evidence of droplet burning and gas-phase combustion with many similarities to micrometer-scale aluminum combustion. Detached diffusion flames could be seen surrounding the particles and nanofeatures were observed in the quenched particles. The nanofeatures are a result of condensation from gas phase combustion. Although not shown, energy dispersive X-ray spectroscopy (EDX) analysis was conducted on both the large parent (greater than 1 μm) particles and the nanofeatures, which confirmed the presence of aluminum and oxygen suggesting that the particles contained at least some portion of aluminum oxide. No nitrogen was detected in the EDX analysis although it has been observed by other researchers (Il'in et al., 2001) investigating aluminum hydride combustion in air.

CONCLUSIONS

The effects of pressure on the ignition behavior of aluminum hydride in air were examined at heating rates of 1×10^5 K/s for pressures ranging from atmospheric to about 7 MPa. We find that ignition temperature was approximately linearly dependent on pressure from atmospheric conditions to about 0.4 MPa. Above 0.4 MPa the ignition temperature was approximately constant with an average value of 760 K. This result suggests that the dehydrogenation process of aluminum hydride is independent of pressure under the conditions tested. In fact, this average ignition temperature is only 40 K higher than the previously established dehydrogenation temperature of aluminum hydride under vacuum conditions at this heating rate.

A transition in ignition behavior was observed coinciding with the constant ignition temperature regime above 0.4 MPa. Broadband light emission transitioned from very smooth broad behavior to very sharp and abrupt behavior suggesting a rapid change in mechanistic behavior. At the same time, shadowgraph high-speed imaging showed a very distinct change in gaseous behavior in the form of well-defined density gradients above 0.4 MPa. These two results, along with a constant ignition temperature over a large range of pressure, suggest two possibilities: (1) kinetic behavior became faster than the diagnostics used, or (2) autoignition or even explosion of H_2/air mixtures was occurring during the ignition process.

Finally, once the aluminum component of the aluminum hydride was visibly ignited, it demonstrated many of the same features, which have been observed with traditional

aluminum combustion. For instance, detached diffusion flames were observed with individual particles; spinning, jetting, smoke trails, and even particle fragmentation or explosion were all observed with high speed imaging. Post-mortem inspection of quenched particles also verified gas phase combustion with the presence of nanofeatures, which were clearly a result of condensation from the gas phase.

ACKNOWLEDGMENT

FUNDING

REFERENCES

Ahluwalia, R.K., Hua, T.Q., and Peng, J.K. 2009. Automotive storage of hydrogen in alane. *Int. J. Hydrogen Energy*, **34**, 7731–7740

Bazyn, T., Eyer, R., Krier, H., and Glumac, N. 2004. Combustion characteristics of aluminum hydride at elevated pressure and temperature. *J. Propul. Power*, **20**(3), 427–431.

Bazyn, T., Krier, H., and Glumac, N. 2005. Oxidizer and pressure effects on the combustion of 10-mm aluminum particles. *J. Propul. Power*, **21**(4), 577–582.

Bazyn, T., Krier, H., Glumac, N., Shankar, N., Wang, X., and Jackson, T.L. 2007. Decomposition of aluminum hydride under solid rocket motor conditions. *J. Propul. Power*, **23**(2), 457–464.

Beckstead, M.W. 2005. Correlating aluminum burning times. *Combust. Explos. Shock Waves*, **41**(5), 533–546.

Belyaev, A.F., Frolov, Y.V., and Korotkov, A.I. 1968. Combustion and ignition of particles of finely dispersed aluminum. *Combust. Explos. Shock Waves*, **4**(3), 323–329.

Brzustowski, T.A., and Glassman, I. 1964. Vapor-phase diffusion flames in the combustion of magnesium and aluminum: II. Experimental observations in oxygen atmosphere. In *Heterogeneous Combustion*, AIAA, Progress in Astronautics and Aeronautics Series, vol. 15, Academic Press, New York, NY, pp. 117–158.

Bucher, P., Yetter, R.A., and Dryer, F.L. 1996. Flame structure measurement of single, isolated aluminum particles burning in air. *Proc. Combust. Inst.*, **26**(2), 1899–1908.

Bucher, P., Yetter, R.A., Dryer, F.L., Parr, T.P., and Hanson-Parr, D.M. 1998. PLIF species and ratiometric temperature measurements of aluminum particle combustion in O_2, CO_2, and N_2O oxidizers, and comparison with model calculations. *Proc. Combust. Inst.*, **27**(2), 2421–2429.

Bucher, P., Yetter, R.A., Dryer, F.L., Vicenzi, E.P., Parr, T.P., and Hanson-Parr, D.M. 1999. Condensed-phase species distributions about Al particles reacting in various oxidizers. *Combust. Flame*, **117**(1–2), 351–361.

Castro, F.J., and Meyer, J. 2002. Thermal desorption spectroscopy (TDS) method for hydrogen desorption characterization (I): Theoretical aspects. *J. Alloys Compd.*, **330–332**, 59–63.

Connell, T.L., Risha, G.A., Yetter, R.A., Young, G., Sundaram, D.S., and Yang, V. 2011 Combustion of alane and aluminum with water for hydrogen and thermal energy generation. *Proc. Combust. Inst.*, **33**(2), 1957–1965.

Deluca, L.T., Galfetti, L., Severini, F., Rossettini, L., Meda, L., Marra, G., D'Andrea, B., Weiser, V., Calabro, M., Vorozhtsov, A.B., Glazunov, A.A., and Pavlovets, G.J. 2007. Physical and ballistic characterization of AlH_3-based space propellants. *Aerosp. Sci. Technol.*, **11**, 18–25.

Drew, C.M., Gordon, A.S., and Knipe, R.H. 1964. Study of quenched aluminum particle combustion. In *Heterogeneous Combustion*, AIAA, Progress in Astronautics and Aeronautics Series, vol. 15, Academic Press, New York, NY, pp. 17–39.

Friedman, R., and Macek, A. 1963. Combustion studies of single aluminum particles. *Proc. Combust. Inst.*, **9**, 703–712.

Frolov, Y.V., Pokhil, P.F., and Logachev, V.S. 1972. Ignition and combustion of powdered aluminum in high temperature gaseous media and in a composition of heterogeneous condensed systems. *Combust. Explos. Shock Waves*, **8**(2), 213–236.

Gordon, A.S., Drew, C.M., Prentice, J.L., and Knipe, R.H. 1968. Techniques for the study of the combustion of metals. *AIAA J.*, **6**(4), 577–583.

Graetz, J., and Reilly, J.J. 2005. Decomposition kinetics of the AlH_3 polymorphs. *J. Phys. Chem. B*, **109**, 22181–22185.

Graetz, J., and Reilly, J.J. 2006. Thermodynamics of the α, β, and γ polymorphs of AlH_3. *J. Alloys Compd.*, **424**, 262–265.

Graetz, J., Reilly, J.J., Kulleck, J.G., and Bowman, R.C. 2007. Kinetics and thermodynamics of the aluminum hydride polymorphs. *J. Alloys Compd.*, **446–447**, 271–275.

Hu, E., Huang, Z., He, J., and Miao, H. 2009. Experimental and numerical study on laminar burning velocities and flame instabilities of hydrogen-air mixtures at elevated pressures and temperatures. *Int. J. Hydrogen Energy*, **34**, 8741–8755.

Il'in, A.P., Bychin, N.V., and Gromov, A.A. 2001. Products of combustion of aluminum hydride in air. *Combust. Explos. Shock Waves*, **37**(4), 490–491.

Ismail, I.M.K., and Hawkins, T. 2005. Kinetics of thermal decomposition of aluminum hydride: I-non-isothermal under vacuum and in inert atmosphere (argon). *Thermochim. Acta*, **439**, 32–43.

Kruetz, T.G., and Law, C.K. 1996. Ignition in nonpremixed counterflowing hydrogen verses heated air: Computational study with detailed chemistry. *Combust. Flame*, **104**(1–2), 157–175.

Kuryavtsev, V.M., Sukhov, A.V., Voronetskii, A.V., and Shpara, A.P. 1979. High-pressure combustion of metals (three zone model). *Combust. Explos. Shock Waves*, **15**(6), 50–57.

Law, C.K. 1973. A simplified theoretical model for the vapor-phase combustion of metal particles. *Combust. Sci. Technol.*, **7**(5), 197–212.

Lewis, B., and Von Elbe, G. 1987. *Combustion, Flames and Explosions of Gases*, 3rd ed., Academic Press, New York.

Macek, A. 1967. Fundamentals of combustion of single aluminum and beryllium particles. *Proc. Combust. Inst.*, **11**, 203–217.

McBride, B.J., and Gordon, S. 1996. *Computer Program for Calculation of Complex Equilibrium Compositions and Applications II*, NASA Reference Publication 1311, Washington, D.C.

Sakintuna, B., Lamari-Darkrim, F., and Hirscher, M. 2007. Metal hydride materials for solid hydrogen storeage: A review. *Int. J. Hydrogen Energy*, **32**, 1121–1140.

Sartori, A., Istad-Lem, A., Brinks, H.W., and Hauback, B.C. 2009. Mechanochemical synthesis of alane. *Int. J. Hydrogen Energy*, **34**, 6350–6356.

Shark, S.C., Pourpoint, T.L., Son, S.F., and Heister, S.D. 2013. Performance of dicyclopentadiene/H_2O_2-based hybrid rocket motors with metal hydride additives. *J. Propul. Power*, **29**(5), 1122–1129.

Son, S.F., Dye, R.C., Busse, J.R., Sandstrom, M.M., Oschwald, D.M., and Janicke, M.T. 2003. Combustion of nanoaluminum in air. In *Proceedings of JANNAF Subcommittee Meeting*, Colorado Springs, CO, December 1–5; Chemical Propulsion Information Agency, Columbia, MD.

Young, G., Piekiel, N., Chowdhury, S., and Zachariah, M.R. 2010a. Ignition behavior of α-alane. *Combust. Sci. Technol.*, **182**(7), 1341–1359.

Young, G., Risha, G.A., Miller, A.G., Glass, R.A., Connell, T.L., and Yetter, R.A. 2010b. Combustion of alane-based solid fuels. *Int. J. Energetic Mater. Chem. Propul.*, **9**(3), 249–266.

Zheng, X.L., and Law, C.K. 2004. Ignition of premixed hydrogen/air by heated counterflow under reduced and elevated pressures. *Combust. Flame*, **136**(1–2), 168–179.